Closing the Contrast Gap between Testbed and Model Prediction with WFIRST-CGI Shaped Pupil Coronagraph

Hanying Zhou*, Bijan Nemati, John Krist,
Eric Cady, Camilo Mejia Prada, Brian Kern, Iyla Poberezhsky
Jet Propulsion Laboratory, California Institute of Technology
4800 Oak Grove Drive, Pasadena, CA 91109 USA

ABSTRACT

JPL has recently passed an important milestone in its technology development for a proposed NASA WFIRST mission: demonstration of a better than $1x10^{-8}$ contrast over broad bandwidth (10%) on both shaped pupil coronagraph (SPC) and hybrid Lyot coronagraph (HLC) testbeds with WFIRST telescope optics. Challenges remain, however, in the technology readiness for the proposed mission. One such is the discrepancy between the achieved contrast on testbeds and their corresponding model predictions. A series of testbed diagnosis and modeling activity were planned and (some) carried out on SPC testbed in order to close the gap. A very useful tool we developed was to analyze the measured testbed Jacobian and compare with its model version that was used to control image plane speckle pattern. The difference between these two is the error in the control Jacobian. When the error, which includes both amplitude and phase, was inserted into a separate prediction model with nominal Jacobian, the model prediction became closely matching the SPC testbed behavior in both contrast floor and contrast convergence speed. This offers a new perspective and is a step closer toward model validation for high contrast coronagraph. Further Jacobian analysis and modeling provided clues to the possible sources for the mismatch: the DM misregistration and the underrepresented testbed optics wavefront error (WFE) and the deformable mirror (DM) setting for correcting this WFE. These analyses suggested that high contrast coronagraph has a tight tolerance in the accuracy of its control Jacobian. Modifications to both testbed control model as well as prediction model are being implemented and future works discussed.

Key words: Model validation, high contrast coronagraph, shaped pupil coronagraph, EFC, wavefront sensing and control, Jacobian matrix, diffraction modeling, WFIRST-CGI, space telescopes

1. INTRODUCTION

SPC is one of the two baseline architectures in current coronagraph instrument (CGI) design that is under intense development as a part of a proposed Wide-Field InfraRed Survey Telescope (WFIRST) mission [1- 5]. JPL has recently passed Milestone 5 (MS5) in its series of technology demonstrations in which the contrasts of both SPC and HLC have been demonstrated to be better than $1x10^{-8}$ over a broad bandwidth (10%) [2, 3]. Challenges remain, however. Among them, the discrepancy between the achieved contrast on testbed and its model prediction is of major concern. As shown in Figure 1, at the time of MS5 passage, the average contrast over dark hole (DH) region from several testbed runs was around $8.4x10^{-9}$ for SPC, while a PROPER [6] based model prediction was close to $2.4x10^{-9}$ (with estimated pupil WFE, mostly from shaped pupil mask), a roughly 3.5 times in contrast discrepancy. Additionally the contrast convergence speed was also vastly different: on testbed it took over hundreds iteration; the model, on the other hand, typically achieves its predication in about a few tens iterations.

Model validation for high contrast (e.g. $1x10^{-9}$) coronagraph proved to be very challenging in the past, due to many difficulties and complications in testbed environment [7, 8]. Fundamentally it is difficult to introduce calibrated effects at desired contrast level for test: either too little at $\sim1x10^{-10}$ level, like dead or pegged actuators, dark hole sizes, mask errors, etc.; or too much at $\sim1x10^{-7}$ level, like particle spots. Additionally, poor understanding and estimation of incoherent light presented in the speckle complicated the wavefront control and thus limited the achievable contrast on the testbed. As a result, only moderate successes demonstrated in predicting the contrast sensitivity such as occulter mask translation, while predicting contrast floor remains to be an elusive goal [8].

*hanying.zhou@jpl.nasa.gov

To close the performance gap, a number of testbed diagnosis and modeling activity were planned after MS5 passed and partially carried out before it was decommissioned shortly afterward. This included examinations of: 1) DM actuator poke response, or Jacobian; 2) changes in testbed optics layout (distance) versus model assumed; 3) system WFEs, particularly the low order WFE of shaped pupil mask; and 4) distortion in shaped pupil mask amplitude, among others. All of these were thought to be potentially sensitive in reaching designed contrast.

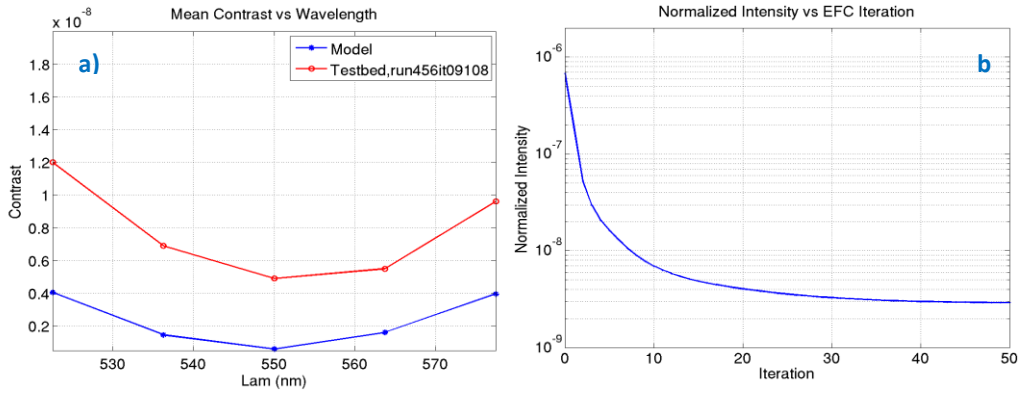

Figure 1. At the time of Milestone 5 passage: a) The predicted contrast (blue) is about 3.5x better than testbed achieved. b) The predicted contrast convergence speed was at a few tens of iterations, faster than testbed's hundreds

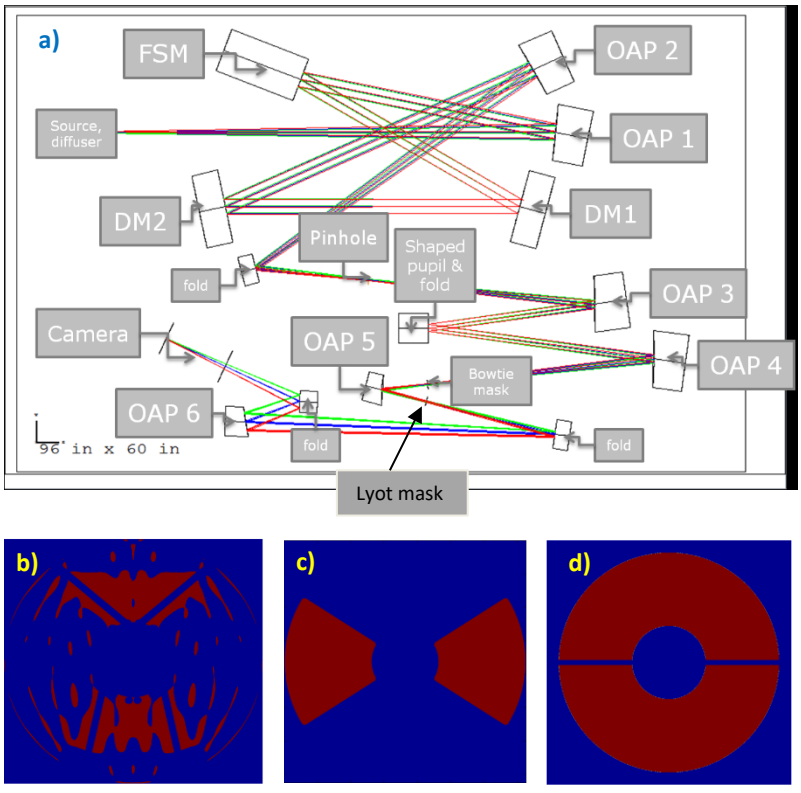

Figure 2. Upper a) SPC testbed layout schematic. FSM: fast steering mirror, OAP: off-axis parabola, Bottom: shaped pupil Lyot coronagraph masks used for MS5, b) shaped pupil mask (SPM), c) occulter mask, and d) Lyot stop mask; testbed has circular entrance pupil

The first thing we noticed was some inconsistencies between testbed layout (schematic shown in Figure 2a) specifications and model prescription. For example, DM1 was off pupil location (by design) by a large amount (~230mm). While the error sounded significant, the improvement after this being corrected in testbed control model turned out to be insignificant in post EFC contrast (This was not totally surprising given the iterative nature of wavefront control to correct imperfections in a system).

Another early focus was on better estimation of system low-order WFE (which mostly comes from shaped pupil mask manufactured). Some earlier modeling of testbed PSF versus focus scan behavior (in terms of PSF peak, peak-to-sidelobe ratio, as well as PSF pattern) showed that the model was reasonably matched to testbed results only after incorporating a trial-and-error pupil WFE (comparable to testbed estimation). Better representation of this WFE in model would improve the match further, but trial-and-error was an inefficient way to find this knowledge. However it was also difficulty to improve the pupil WFE estimation accuracy from phase retrieval measurement when a shaped pupil mask was in use which, as shown in Figure 2b, has small open area (its large dark horizontal area renders estimation of astigmatism difficult).

Our effort was subsequently concentrated on examining the testbed Jacobian. Instead of merely spot checking on a few actuators as it had been done occasionally in the past, we called to perform a survey of as many active actuators as possible. The data collection was somewhat time consuming (about a weekend), but the result can give a better picture as to how well testbed matches the model prescription.

In the following, after a brief explanation of Jacobian and its testbed measurement method, we present our analysis result of the collected testbed Jacobians. The significance of the Jacobian error (the difference between measured Jacobian and model Jacobian) is then modeled by inserting the error into a predication model. This is followed by modeling the potential sources of the Jacobian error. A summary and discussion is included afterward.

2. JACOBIAN IN EFC WAVEFRONT CONTROL AND TESTBED MEASUREMENT

Most WFIRST coronagraph integrated modeling at JPL uses a PROPER based full diffraction model to compute image plane speckle pattern [6, 9], where beam is propagated from surface to surface according to their physical distances. High contrast imaging testbeds (HCITs) at JPL, on the other hand, uses a mostly FFT based ('compact') model to speed up control execution (the only Fresnel propagation used is from DM1 to DM2). Over the time, our prediction model for this work also used a compact version. Besides the computation time benefit, the main other reason was to simplify the comparison of Jacobian phase. Due to long Fresnel propagation and small beam size from Lyot stop to final camera location of the SPC tested optics layout, the electric field in the full model is modified by a strong off-the-center phase term, which has no effect on contrast.

The wavefront control method in both model prediction and testbed used Electric Field Conjugation (EFC) algorithm to minimize image plane speckle pattern [10, 11]. The control matrix, typically termed Jacobian or G matrix, is a collection of G_k, the linear approximation of image plane electric field response to each actuator's (pupil plane) unit strength poke (difference between poked field and base no-poke field):

$$G_k = C\left\{E_{pup} e^{i\phi_{dm,k}}\right\} - C\left\{E_{pup}\right\} \approx iC\left\{E_{pup}\phi_{dm,k}\right\} \tag{1}$$

where C denotes the linear coronagraph operator, E_{pup} is pupil plane electric field, $\phi_{dm,k}$ is kth actuator's unit poke piston. In EFC algorithm G is commonly arranged by its real and imaginary parts of the electric field, pixel by pixel (of dark hole), and wavelength by wavelength (in broadband dark hole correction), in different rows; and actuator by actuator in different columns. Weighting for emphasizing different part of dark hole or different wavelength can be applied to each individual G_k. Once G (the matrix collection of G_k) is established and dark hole field E_{DH} is sensed, the DM correction needed at each iteration is then:

$$\begin{bmatrix} a_1 \\ \vdots \\ a_k \end{bmatrix} = \begin{bmatrix} \Re\{G_1\} & \dots \Re\{G_k\} \\ \vdots & \vdots \\ \Im\{G_1\} & \dots \Im\{G_k\} \end{bmatrix}^{-1} \begin{bmatrix} \Re\{iE_{DH}\} \\ \vdots \\ \Im\{iE_{DH}\} \end{bmatrix} \tag{2}$$

Often regularization β is added to damp the imperfect correction due to linear approximation to a nonlinear problem, imperfect sensing, as well as imperfect system calibration. One way of doing this can be:

$$G_{inv} = \left[G^T G + \beta \cdot \max\left(diag\left(G^T G \right) \right) \cdot I \right]^{-1} G^T, \quad a = G_{inv} \cdot E_{DH} \tag{3}$$

How well the speckle field correction at each step depends on the accuracy of control Jacobian G matrix *(*or its inverse G_{inv}) and the accuracy of sensing E_{DH}, and our focus in this paper was on the former (our another paper [12] focused on the later). In many close loop iterative control applications (e.g., adaptive optics), small imperfections in DM control mechanism may not be very important, as they will be corrected together with other system WFE given enough iterations. In high contrast coronagraph such as in WFIRST, where both achievable DH contrast floor and contrast convergence speed matter, tolerance in Jacobian imperfectness could be much tighter; high accuracy in Jacobian is key to achieve desired contrast floor in a reasonable amount of time.

To measure the Jacobian G_k of each actuator, which contains both amplitude and phase, the simplest method is to use the same pair-wise DM probing scheme used for dark hole electric field estimation during wavefront control [11]:

$$I_j^{+/-} = \left| E_G \pm \Delta P_j \right|^2 + I_{inc} = \left| E_G \right|^2 + \left| \Delta P_j \right|^2 \pm 2\Re\left\{ E_G^* \Delta P_j \right\} + I_{inc} \tag{4}$$

where ΔP_j is the probing field added to the existing to-be-measured DM poke field $E_G = C\{\ \}$, and I_j are intensities measured as a result of jth probe, either positive (+) or negative (-). From Eq. (4), one has:

$$\Delta I_j \equiv I_j^+ - I_j^- = 4\Re\left\{ E_G \Delta P_j \right\} \tag{5}$$

or in the form of matrix for N pair of probes [11]:

$$\begin{bmatrix} \Delta I_1 \\ \vdots \\ \Delta I_N \end{bmatrix} = 2 \begin{bmatrix} -\Im\{\Delta P_1\} & \Re\{\Delta P_1\} \\ \vdots & \vdots \\ -\Im\{\Delta P_N\} & \Re\{\Delta P_N\} \end{bmatrix} \begin{bmatrix} \Re\{E_G\} \\ \Im\{E_G\} \end{bmatrix} \tag{6}$$

Here ΔP_i are image plane field due to probe applied and are obtained by propagating the coronagraph model with the probing field. One can then find the speckle pattern for each pixel with measured N intensity pairs based on Eq. (6). G_k is then obtained as the difference between poked field and base no-poke field.

On SPC testbed, total of 3 pairs of positive-negative DM probes plus a no-probe images were used. This was to improve ill-conditioning due to noise in the inversion of Eq. (6) and to remove incoherent background. Also, instead of real and imaginary parts of Jacobian, the processed measured Jacobian data used amplitude and (wrapped) phase components of Jacobian. The reason was that the former was directly measured as $\sqrt{\left(I_j^+ - I_j^-\right)/2 - I_o}$, while the latter was derived from intensity measurement and Eq. (6).

For control Jacobian, simple forward propagation of delta DM poke was calculated with the coronagraph propagation model based on Eq. (1). The result was also arranged into amplitude and phase, for easy comparison with measured Jacobian.

3. TESTBED JACOBIAN ERROR AND ITS IMPACT ON CONTRAST

3.1 Jacobian error distribution

Using above method, a little over 700 (out of ~1200 total) actuators (that were considered strong enough) testbed measured Jacobian and control Jacobian were collected at near dark hole DM setting. Figure 3 shows an example of one actuator's Jacobian, measurement versus its model. Here we used two metrics to quantify the Jacobian error: difference in mean amplitude over dark hole region in percentage (upper rightmost in Fig. 3), and difference in phase (in x and y components) as tilt gradient ($\Delta\phi_{\text{per } \lambda/D}$). Collect each actuator's error and compose them according to their locations, we have a distribution of testbed Jacobian error 2D map as shown in Figure 4.

Ignoring the edge actuator errors (which tend to be unreliable due to weak response caused large measurement error), we saw that both DMs' measured Jacobian amplitudes were about ~25% lower than expected on average. On the phase part, the error was roughly on the order of 0.05 rad per λ/D, and the distribution was not of random nature but of certain pattern, indicating possible systematic error in control Jacobian.

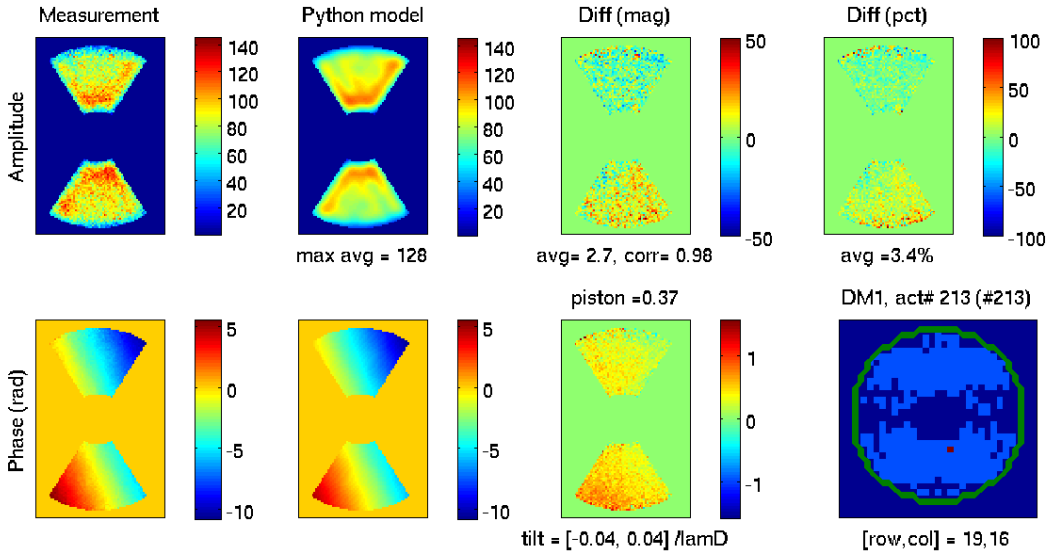

Figure 3. An example of testbed measured Jacobian and its model version: top row shows amplitudes and their difference, (meas-model), and in percentage of difference (*pct*), (meas-model)/model. Bottom row shows phases and their difference (in rad). Tilt values are estimated phase difference gradient (per λ/D) of x and y components. Also shown the actuator location being poked (red dot) against all active actuators (light blue)

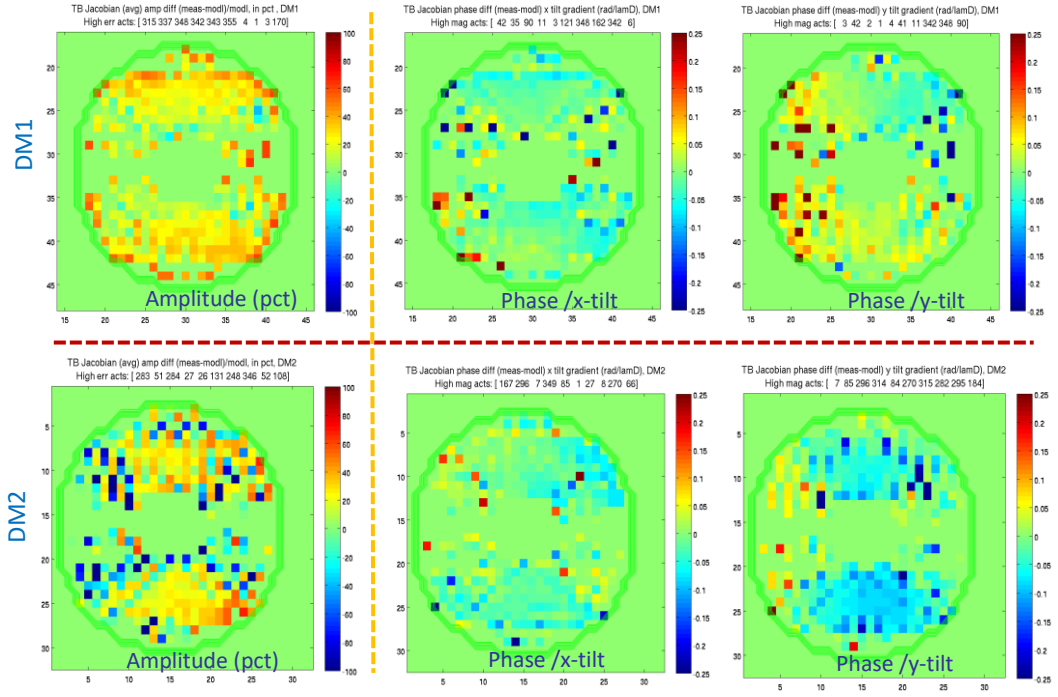

Figure 4. Jacobian error distribution arranged in actuator's DM location. Upper row: DM1; bottom row: DM2. Left column: amplitude error in % (*pct*); right two columns: phase error gradient per λ/D of x and y components

A little note here: though the Jacobian as measured was close enough to its model version for actuators in open area, most actuators at edges (and for WFIRST SPC there are many of these, due to SPM's many thin edges, see Figure 2b) were noisy in raw data and deemed not reliable. It is therefore infeasible to directly use measured Jacobian for actual wavefront control (which would alleviate all the mismatch problem). Nevertheless, the measurement did paint a global picture of Jacobian error that can offer many clues to testbed problem.

3.2 Impact of Jacobian error on contrast floor and contrast convergence

With the Jacobian error as described above: about ~25% in average amplitude mostly underrepresented in control model, and a phase error in tilt gradient on the order of 0.05 rad per λ/D, our first question was if the observed Jacobian error significant in limiting testbed contrast?

To answer this, we imported the Jacobian error into a separate predication model to see its impact on contrast performance. We adjusted each of our prediction model's nominal Jacobian, G_k, to carry the testbed error as:

$$G_{k,TB} = \frac{1}{1+pct_k} G_k e^{\Delta\phi_x \cdot x + \Delta\phi_y \cdot y} \qquad (7)$$

That is, its amplitude was scaled down (pct_k is the percentage error shown in left column of Figure 4, and its phase was modified by adding the phase error (the *x*- and *y*- components of tilt gradient of right two columns of Figure 4. Any actuators whose magnitude errors exceed 2σ in error histogram would remain unadjusted in magnitude. Similarly, any actuators whose phase errors exceed 2σ remain unchanged in phase. This was to minimize impact caused by spurious measurement error.

We then carried out EFC wavefront control with above error ridden Jacobian and an estimated low-order pupil WFE of ~60nm rms (estimated from fitting PSF focus scan data). The WFE has Zernike coefficients roughly at a level of ~λ/10 RMS or λ/2 PV for focus and astigmatism terms: *Z4~Z7* = [-45 -40 -10 2] nm rms, comparable to testbed estimation.

The result, as shown in Figure 5, strongly suggested that the level and nature of Jacobian error could be largely responsible for the observed SPC testbed contrast behavior: when both amplitude and phase error included, the prediction model took about ~120 iterations to reach a contrast floor about 8×10^{-9}, similar to MS5 testbed result [3, 4], compared with a no-error nominal model which would need only ~ 40 iterations to reach 2.4×10^{-9} contrast. The trial-and-error optimal regularization that gave the best EFC result was found to be $\beta = 1.2\times10^{-2}$, also very close to what testbed found and used.

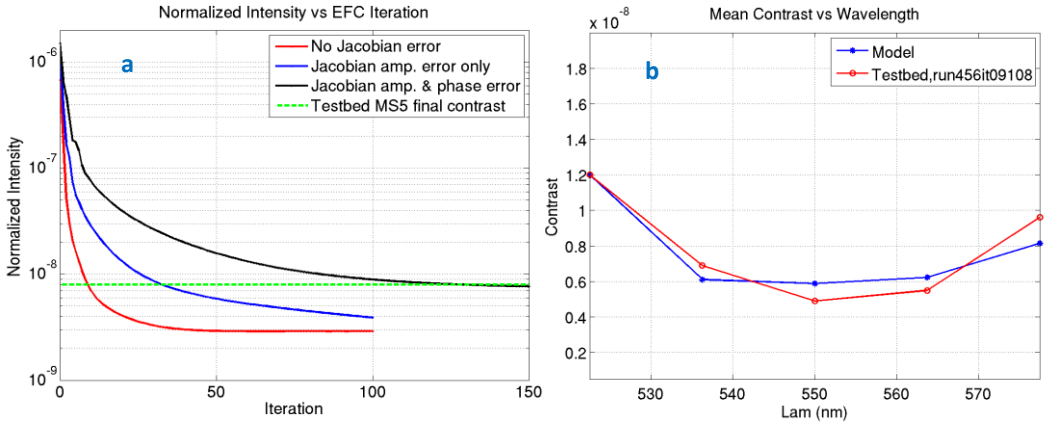

Figure 5. Impact of observed Jacobian error on SPC testbed contrast: a) The Jacobian error appears to set the contrast floor as well as its convergence speed. b) The final contrast has similar wavelength dependency to MS5 result.

It is worth noting that, the amplitude error, which was thought to be relatively easy to fix, mostly slowed down the contrast convergence but did not appear to be contrast floor setting. In other words, to improve contrast floor, it is more important to minimize Jacobian phase error as much as possible.

4. SOURCES OF JACOBIAN ERROR

Given the significance of Jacobian error on dark hole contrast, our next question was what led to these errors? This is harder to answer but important if we were to improve our testbed result, which is the ultimate goal. Here we present some analysis that provides some clues to this question.

4.1 Jacobian phase error and DM registration offset

One naturally links Jacobian phase error to DM offset, since image plane phase tilt is related to pupil plane displacement by (the two are Fourier Transform pair):

$$offset = \frac{\lambda}{2\pi}\Delta\phi = \frac{D}{2\pi}\Delta\phi_{per\,\lambda/D} \qquad (8)$$

We can easily convert the Jacobian phase error into DM registration error. The result is shown in Figure 6, where left two columns are the cleaner version of the right two columns of Figure 4 (with outliers >2σ removed) but now in unit of um. The mean (absolute) offset magnitude is over ~200um (while mean rigid DM misalignment ~150um), about testbed alignment uncertainty range.

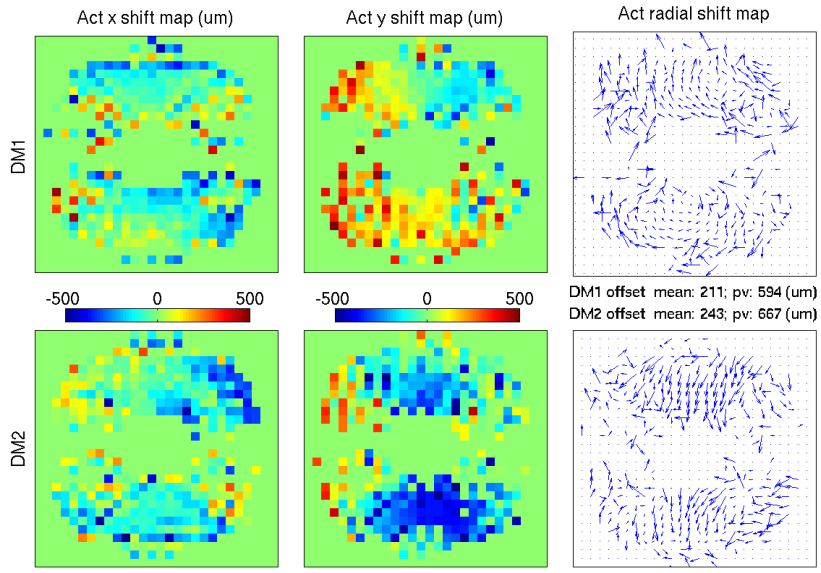

Figure 6. DM registration error derived from Jacobian phase error: left two columns are actuator x- and y- offset in um (from calibrated grid map); right column is a (upside down flipped) offset quiver plot

If we treat DM registration offset as a result of a wavefront slope, we can reconstruct its corresponding "WFE" through a Shack-Hartman method. The result is shown in Figure 7, which can be thought of the impact distribution of individual actuator misregistration on Jacobian phase modification. Again, both DMs show large mean shift, and some focus and astigmatism.

While it is straightforward to link Jacobian phase error to DM offset, understanding the full reason for the offset is little trickier than it appears to be. The tip/tilt in the phase error (or the mean *x*- and *y*- shift in converted DM offsets) can be readily interpreted as misalignment of rigid DM vs pupil, which were roughly at level of 5~15% actuator unit (50~150um). In fact it was verified that there was a shift in DM registration after shaped pupil mask (SPM) replaced

its surrogate flat (DM registration data was taken with a flat in place of SPM) due to 1 mm thickness difference between SPM and the surrogate flat. On the other hand, the focus (the equivalent grid spacing change) and astigmatism terms in DM offset "WFE" were not entirely understood, except that they were unlikely from actual physical grid distortion. We suspected that they could be related to testbed WFE (which contains some focus and astigmatism terms) and its DM LOWFE setting (see Sect 4.2 below). More modeling works are needed to precisely answer this.

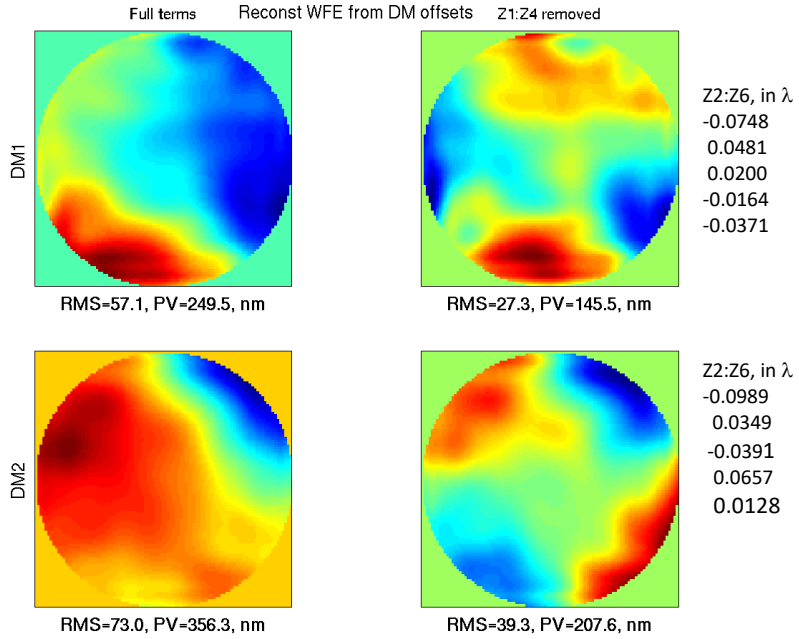

Figure 7. Impact distribution of DM registration error on Jacobian phase. Left: full impact; right: mean shift and grid spacing error (tip tilt focus) removed

4.2 Jacobian magnitude error and system WFE and LOWFE DM setting

For amplitude error, the natural first reaction was to look more carefully over DM gain calibration. Small inconsistency in photometric normalization was found in testbed control model. Then influence function for DM2, which was assumed to be the same as DM1 but never actually measured, was updated which turned out to be slightly different from (fattier than) that of DM1. Early Jacobian measurement data itself was also discovered to be unreliable, particularly DM2, due to the use of large poke voltage (20 Voltage measurement unit (VMU), equivalent of 80nm poke piston, in an effort to boost measurement accuracy for weak actuators), which caused saturation and strong nonlinearity. After discovered this and reduced poke voltage to 2VMU, the measured Jacobian of actuators in open area were of much reasonable quality (at the price of edge actuators' quality).

However, after all these corrections and improvement, we were still not able to explain the level of Jacobian amplitude off seen in the Jacobian data shown in Fig.4, and decided to check if DM's LOWEF setting to correct system WFE has any effect.

Recall that in Eq. (1), Jacobian is a linear approximation of image plane electric field response to pupil plane unit strength DM poke. It is often calculated with WFE free version of coronagraph propagation in model and with an assumption that the poke strength is small (which we term it nominal Jacobian in this paper). When there is non-insignificant DM stroke set to correct system pupil WFE, the true Jacobian could differ from its no WFE small poke version where linearity approximation holds better. At a larger WFE φ_{pup} and a corresponding DM setting $\phi_{dm,w}$ case, instead of linear approximation in Eq. (1), one would now have:

$$G_k = C\left\{E_{pup}e^{i\varphi_{pup}}e^{i\left(\phi_{dm,w}+\phi_{dm,k}\right)}\right\} - C\left\{E_{pup}e^{i\varphi_{pup}}e^{i\phi_{dm,w}}\right\}$$
$$\approx C\left\{iE_{pup}\,\phi_{dm,k} - E_{pup}\,\phi_{dm,k}\left(\varphi_{pup}+\phi_{dm,w}\right)\right\} \quad (9)$$

after omitting third order or higher terms as well as second order term $\phi^2_{dm,k}$ ($\phi_{dm,k}$ is much smaller compared with ϕ_w and φ_{pup} for a large WFE case). $\phi_{dm,w}$ would partially cancel out φ_{pup} (the two have opposite sign in general) but not fully, even when Jacobian is calculated or measured when dark hole is nearly reached; since the goal in coronagraph is not to minimize pupil WFE but to redistribute (the high order component of) it such that it will result in a desired dark hole region in image plane. Often Jacobian is calculated or measured far from the coronagraph reach to the dark hole solution. In any case the second term in Eq. (9) will change Jacobian amplitude and its phase relative to its nominal version. Since $\phi_{dm,k}$ is zero except the kth actuator being poked (for Jacobian purpose), only local values of $\phi_{dm,w}$, φ_{pup} matter (although in reality actuator has a finite span of influence function, but for this analysis we use a delta like influence function for simplicity). Their effect is to add approximately a (quadrature phase shifted) copy of (nominal) field response with an attenuated amplitude, whose attenuation is roughly proportional to the residual of the imperfect DM cancellation to pupil WFE at kth actuator location $\varphi_{pup}+\phi_{dm,w}$. And Jacobian amplitude error (in percentage) relative to its nominal one would be:

$$err_{amp} \approx 100*\left(\sqrt{1+\left(\varphi_{pup}+\phi_{dm,w}\right)^2}-1\right) \quad (10)$$

The nominal Jacobian phase will be modified by a phase term related to this residual also:

$$err_{ph} \approx \varphi_{pup}+\phi_{dm,w} \quad (11)$$

Figure 7 shows the difference between the nominal Jacobian and Jacobian with estimated testbed WFE and its initial DM setting incorporated. The percentage change in Jacobian amplitude between these two, is at the level of around 20% on average, roughly matching observed amplitude discrepancy. Note however, Jacobian amplitude error could be further aggravated if this residual is coupled with DM registration error.

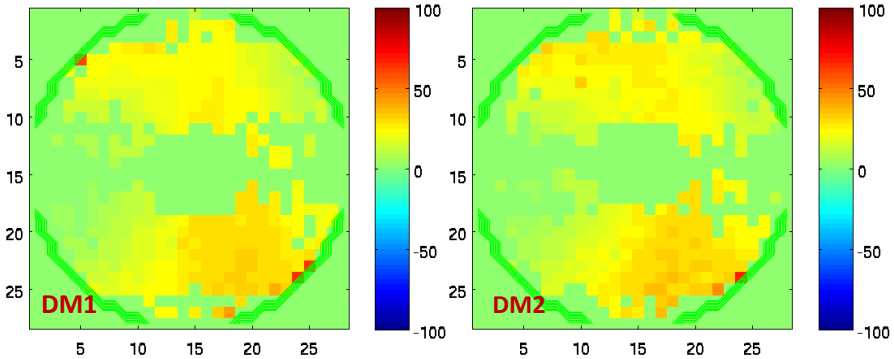

Figure 7. Amplitude difference (in %) in a nominal Jacobian and a Jacobian incorporating estimated testbed pupil WFE and its initial DM setting. At a level of 25% on average, it roughly matches observed amplitude discrepancy.

From a dynamic perspective, the high order residual WFE after initial flattening (low order WFE control) tends to change little in magnitude as EFC iteration goes ($\phi_{dm,w}$ is mostly to redistribute φ_{pup} after low-order WFE flattening). However, the reshape or redistribution of its content could change individual G_k substantially. Traditionally prediction model calculates Jacobian once and does not dynamically update it during EFC run to reflect DM change. This may not matter for well-built system with small high order WFE. If there is large high-order WFE in coronagraph, it is better to include WFE and its DM setting in the Jacobian calculation and update them along the way to match to the true Jacobian both at the beginning and during EFC iterations.

On SPC testbed the control Jacobian was dynamically updated with DM setting (~ every few iterations) but did not include the low order SPM WFE at the time of MS5. This would lead to control Jacobian amplitude error roughly as:

$$err_{amp,TB} \approx 100 * \left(\sqrt{1+\varphi_{pup}^2} - 1 \right) \quad (12)$$

For an estimated testbed WFE of 60nm rms, or φ_{pup} = 0.7 rad, the amplitude error is then roughly at 22%, very close to what was observed. The phase error would be roughly proportional to pupil WFE:

$$err_{ph,TB} \approx -\varphi_{pup} \quad (13)$$

This suggests that the testbed Jacobian phase errors, as shown in Figs. 4 and 6, could be reflecting testbed WFE in certain way, since both DMs' Jacobians phase errors contain focus and astigmatism terms. However, currently we do not fully understand the apparent mismatch in magnitude (both are smaller than Eq. (13) predicted) and sign change. One possibility of the mismatch could be the bias error in measurement. Unlike amplitude which was "direct" measurement, the Jacobian phase part was model-derived measurement. When system WFE and its DM setting are large enough but not fully included in estimation model, it could introduce significant bias error in measurement and thereby "distort" the true Jacobian error. More work is needed to better understand the origins of the Jacobian phase and amplitude errors.

5. SUMMARY AND FUTRUE WORK

We developed a very useful tool to diagnose testbed imperfections and close contrast gap between testbed and model prediction for high contrast coronagraph. Our analysis and modeling of SPC testbed Jacobian error strongly suggests that the error in the control Jacobian, about ~25% in amplitude, and 0.05rad per λ/D in phase, appears to be limiting the contrast floor and affecting contrast convergence observed on SPC testbed. Two most likely main sources of these errors come from, among others: 1) failure to fully include WFE and its corresponding DM setting in the model when they were modestly large, and 2) failure to include DM registration error. For high contrast coronagraph, the Jacobian has a much tight tolerance in its imperfection than we initially assumed: a system WFE as small as λ/10 rms could derail nominal Jacobian from linearity approximation; a DM registration error at a level of ~200um mean (absolute) offset (or a rigid DM misalignment at about 50~150um) could degrade its speckle suppression ability significantly, especially when coupled with system WFE. However, more careful modeling work needed to better understand the focus and astigmatism terms in Jacobian phase error seen.

Modifications to both testbed control model as well as prediction model are being implemented and continually evolving. According to Eq. (9), accurate control Jacobian depends on good representation of both system WFE and the DM setting, φ_{pup} and $\phi_{dm,w}$. On testbed DM piston was already regularly updated around the time of MS5 passage but not its misregistration nor the system WFE. After the Jacobian study, a static WFE was included in the control model. It would be better if we could include DM misalignment in the model and update WFE dynamically also if possible (if the initial WFE measurement not accurate enough). Similarly prediction model could do better if it dynamically updates Jacobian to reflect DM setting change during EFC iteration for large WFE case.

Due to decommissioning of the original shaped pupil testbed at JPL shortly after the passage of the Milestone 5, however, we were unable to conduct more test cases afterward to firmly validate this. Nevertheless, the approach described in this paper represents a fresh direction to pursue model validation for high contrast coronagraph, a required technology readiness for a proposed NASA WFIRST mission. At the time of this paper's submission, a new dynamic Occulter Mask Coronagraph (OMC) testbed, which will be used for both future SPC and HLC test in static as well as dynamic environments, is near ready to start speckle nulling. Once fully operative, we will iteratively repeat Jacobian survey and model validating our findings with new data. In addition to incorporating Jacobian error into prediction model for prediction as we have been doing, we also intend to incorporate Jacobian error back into control model (if unable to correct the Jacobian error) and check its benefit in performance enhancement.

Another potential future improvement is to use alternative phase estimation technique. As noted in Sect 4.2, the "measured" Jacobian is in reality a model-dependent measurement: specifically, the Jacobian phase is currently obtained through both intensity measurements AND the coronagraph model itself (the amplitude part can be estimated through pair of intensity measurements without model). The result is that the measured data reflects only "relative" error when compared with testbed's control model. Using the same pair-wise DM probe for wavefront control is one most

convenient method (no additional hardware and/or hardware translation needed). In small WFE and LOWEF DM setting case, where linearity approximation holds better, the system bias from such model depend measurement may be limited. In large WFE and its corresponding DM setting case, this model-dependent measurement could potentially miss out significant bias error. It is possible to use other phase measurement techniques such as Phase Retrieval or sets of pinholes near Lyot stop edge [13 -14]. PR is already in extensive use on testbeds (though is extremely time consuming), and pinhole at Lyot stop edge was also demonstrated previously. Both could be a viable alternative to existing model-dependent Jacobian phase measurement.

ACKNOWLEDGMENTS

This work was performed at the Jet Propulsion Laboratory of the California Institute of Technology, under contract with the National Aeronautics and Space Administration. © 2016 California Institute of Technology.

REFERENCES

[1] D. Spergel, et al., "Wide-Field InfraRed Survey Telescope-Astrophysics Focused Telescope Assets WFIRST-AFTA 2015 Report." https://arxiv.org/abs/1503.03757, (2015)
[2] Poberezhsky, I., et al., "WFIRST-AFTA coronagraph starlight suppression technology progress," Proc. SPIE. 9904, (this conference), (2016)
[3] Cady, E., et al., "Demonstration of broadband wavefront control with a shaped pupil Lyot coronagraph for the WFIRST-AFTA Observatory," Proc. SPIE. 9904, (this conference) (2016)
[4] Cady, E., et al., "Laboratory performance of the shaped pupil coronagraphic architecture for the WFIRST-AFTA coronagraph," Proc. SPIE. 9605,96050B-1 (2015)
[5] Zimmerman, N. T., et al., "Shaped Pupil Lyot coronagraph Designs for WFIRST-AFTA," Proc. SPIE, 9605, 96050A-1 (2015)
[6] Krist, J., "PROPER: An optical modeling program for IDL," Proc. SPIE. 6675, 66750P (2007).
[7] Debes, J. H., et al., "WFIRST-AFTA Coronagraphic Operations: Lessons Learned from the Hubble Space Telescope and the James Webb Space," http://arxiv.org/abs/1511.06277 (2015)
[8] Shaklan, S., et al., "Coronagraph starlight suppression model validation," https://exep.jpl.nasa.gov/files/exep/COMBINEDv5_Milestone%203A%20Final%20Report%20072915.pdf ExEp Technology Milestone #3A Final Report (2015)
[9] Krist, J. et al., "Numerical modeling of the proposed WFIRST-AFTA coronagraphs and their predicted performances," J. Astron. Telesc. Instrum. Syst. 2(1), 011003 (2016).
[10] Give'on A. *et al*, "Broadband wavefront correction algorithm for high-contrast imaging system," *Proc. SPIE*. 6691, 66910A (2007).
[11] Give'on A. *et al*, "Pair-wise, deformable mirror, image plane-based diversity electric field estimation for high contrast coronagraphy," Proc. SPIE. 8151, 815110-2, (2011)
[12] Zhou, H., et al, "Diffraction Modeling of Finite Subband EFC Probing on Dark Hole Contrast with WFIRST-CGI Shaped Pupil Coronagraph," Proc. SPIE. 9904, (2016)
[13] Fienup J., "Phase retrieval algorithms: a comparison," Appl. Opt. 21(15), 2758–2769 (1982).
[14] Give'on A. *et al*, "Electric field reconstruction in the image plane of a high-contrast coronagraph using a set of pinholes around the Lyot plane," *Proc. SPIE*. 8442, 84420B-1 (2012).